

Reconfigurable Intelligent Surfaces with Liquid Crystal Technology: A Hardware Design and Communication Perspective

Alejandro Jiménez-Sáez, Arash Asadi, Robin Neuder, Mohamadreza Delbari, and Vahid Jamali

Abstract—With the surge of theoretical work investigating Reconfigurable Intelligent Surfaces (RISs) for wireless communication and sensing, there exists an urgent need of hardware solutions for the evaluation of these theoretical results and further advancing the field. The most common solutions proposed in the literature are based on varactors, Positive-Intrinsic-Negative (PIN) diodes, and Micro-Electro-Mechanical Systems (MEMS). This paper presents the use of Liquid Crystal (LC) technology for the realization of continuously-tunable extremely large millimeter-wave RISs. We review the basic physical principles of LC theory, introduce two different realizations of LC-RISs, namely reflect-array and phased-array, and highlight their key properties that have an impact on the system design and RIS reconfiguration strategy. Moreover, the LC technology is compared with the competing technologies in terms of feasibility, cost, power consumption, reconfiguration speed, and bandwidth. Furthermore, several important open problems for both theoretical and experimental research on LC-RISs are presented.

Index Terms—Liquid crystal, reconfigurable intelligent surface, intelligent reflective surface, millimeter wave, and 6G.

I. INTRODUCTION

In recent years, there has been considerable interest in Reconfigurable Intelligent Surfaces (RISs), particularly within the context of 6G communications. The potential for significant improvements in communication and sensing capabilities through the use of large, passive, and tunable reflectors has led to the development of theoretical models and algorithms in the wireless communication community [1], [2] and subsequent attention from the microwave community towards the practical implementation of RISs [3].

RISs are planar electromagnetic surfaces comprised of many independently tunable reflecting elements. These reflecting elements can be adjusted externally to modify the phase and, in certain instances, the amplitude of the signal reflected at each element. Through the superposition of reflections from each element, the reflection pattern can be dynamically tuned, eliminating the need for complex decoding, encoding, and processing. While demonstrations of reflectarrays and

A. Jiménez-Sáez and R. Neuder are with the Institute of Microwave Engineering and Photonics at Technical University of Darmstadt, Darmstadt, Germany (e-mail: {alejandrosaez, robin.neuder}@tu-darmstadt.de).

A. Asadi is with the Wireless Communication and Sensing Lab at Technical University of Darmstadt, Darmstadt, Germany (e-mail: aasadi@wise.tu-darmstadt.de).

M. Delbari and V. Jamali are with the Resilient Communication Systems Lab at Technical University of Darmstadt, Darmstadt, Germany (e-mail: {mohamadreza.delbari, vahid.jamali}@tu-darmstadt.de).

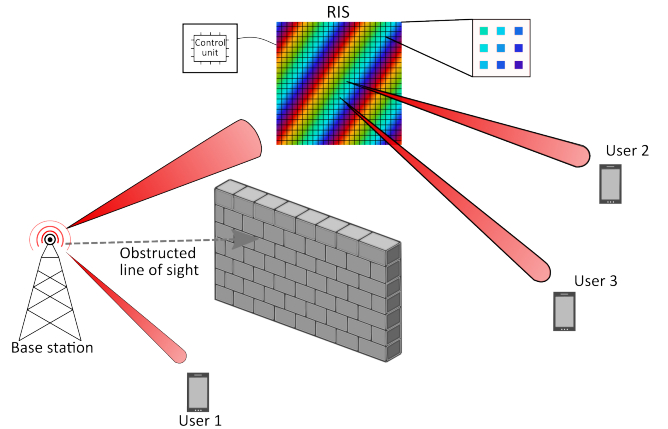


Fig. 1. Example scenario where a RIS establishes a link between a transmitter and two receivers despite an obstacle blocking the LOS path.

predictions on its tunability date back to 1963 [4], their large-scale application to mobile networks (see Fig. 1) has only been recently considered.

So far, various RIS prototypes have been reported in the literature, which mainly employ Semiconductor (SC) technologies (e.g., Positive-Intrinsic-Negative (PIN) diodes [5], varactors [6], Radio-Frequency (RF) switches [7]) to realize the phase shifts. Although a feasible choice of design, their cost and resolution (in case of PIN diodes) can be prohibitive in building truly large and cost-efficient large RISs. An alternative to these technologies is nematic Liquid Crystal (LC) technology. In the last two decades, LCs have been studied for the microwave, millimeter-Wave (mm-Wave), and THz frequency bands [8, Ch. 5]. If fabrication in standard Liquid Crystal Display (LCD) technology is adopted, the manufacturing cost of LC-RISs will be reduced to that of a commercial LCD television. Hence, LC-based designs have the advantages of cost-effective scalability, low energy consumption, and continuous phase shifting, which make them a suitable candidate for realizing extremely large passive RISs. Despite these attractive features, LC characteristics impose new challenges when being integrated into today's mobile communication systems, most notably due to their slow tuning capabilities as compared with SC-RISs.

In this article, we aim at bridging the gap between microwave and antenna design aspects of LC-RISs with mobile communication aspects. To this end, we first review the basic physical principles of LC theory and introduce two different

realizations of LC-RISs, namely the Reflect-Array (RA) and Phased-Array (PhA) methods. Thereby, we particularly highlight their key physical and hardware properties that have a direct impact on the system design and RIS reconfiguration strategy. This is complemented by a concrete comparison against the alternative technologies for building RISs (i.e., SCs and Micro-Electro-Mechanical Systems (MEMS)) in terms of feasibility, cost, power consumption, reconfiguration speed, and bandwidth. Finally, we delve into the challenges of LC-RISs (slow response time, temperature dependencies, bandwidth) and present potential directions for both theoretical and experimental research in order to overcome these challenges.

II. LIQUID CRYSTAL-BASED RIS

In this section, we first present the basic operating principles of LC technologies. Subsequently, we introduce two of the existing LC-RIS implementations, as well as the hardware components required for implementing them.

A. Basic physical principles of LC technology

Phase shifting capability: The working principle of LC is based on its electromagnetic anisotropy¹. In particular, due to the ellipsoidal shape of LC molecules, the LC presents a larger permittivity (i.e., higher phase shift) when the electric field, \vec{E}_{RF} , is aligned with the major axis of the molecules, \vec{n} , than when it is aligned with the minor axis (i.e., lower phase shift), see Fig. 2. Therefore, by controlling the orientation of LC molecules, we can alter the phase shift of the RF signals.

This is achieved by placing a thin LC-layer between two electrodes. Thereby, when no voltage is applied, the molecules are in their relaxed phase, where \vec{E}_{RF} is perpendicular to \vec{n} , and hence LC shows a minimum permittivity $\varepsilon_{r,\perp}$. In contrast, when the maximum voltage is applied, the LC molecules orient along the induced external electric field, which leads to \vec{E}_{RF} being now parallel to \vec{n} and hence a maximum permittivity of $\varepsilon_{r,\parallel}$. The maximum achievable phase shift, $\Delta\theta_{\max}$, therefore scales with $\Delta\varepsilon = \varepsilon_{r,\parallel} - \varepsilon_{r,\perp}$. The LC-layer permittivity and the corresponding maximum achievable phase-shift are dependent on the operating frequency as well as temperature, cf. Fig. 2, which will be elaborated further in Section IV.

Response time: The alignment of the LC along the electrodes when applying a voltage (for positive phase shifts) is faster than the alignment of the molecules due to mechanical anchoring forces (for negative phase shifts). For this reason, usually the latter slow transition is considered and modelled by the decay or switch-off response time, τ_{off} , which is proportional to $\tau_{\text{off}} \propto \gamma_{\text{rot}} d_{LC}^2 / K_{11}$, where γ_{rot} is the rotational viscosity, d_{LC} is the LC-layer thickness, and K_{11} is the splay deformation factor of the LC. Therefore, the response time can be reduced by adopting a narrower LC layer; however, this implies more delicate (hence costly) manufacturing and higher conductor losses, motivating research to reduce losses in thin phase shifters [9]. The LC thickness, d_{LC} , can be as low as a few μm for switch-off response times, τ_{off} , in the order of tens of milliseconds.

¹LC molecules exhibit different electromagnetic properties depending on their relative orientation with the RF electric field.

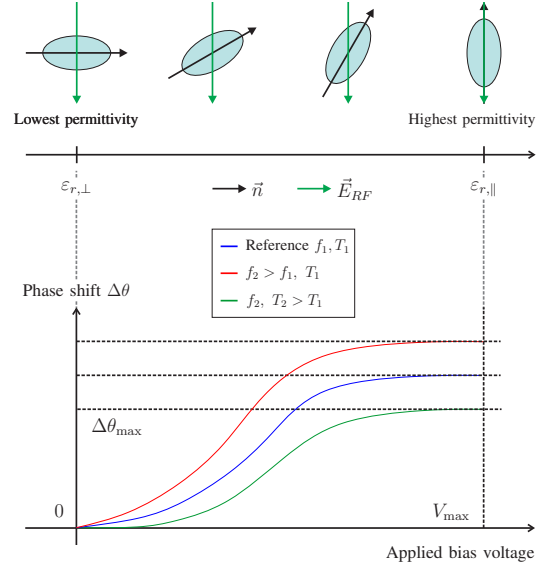


Fig. 2. Top figure: Observed LC permittivity depending on the orientation between the RF electric field, \vec{E}_{RF} , and the LC molecule major axis, \vec{n} . The lowest permittivity, $\varepsilon_{r,\perp}$, is observed when \vec{E}_{RF} and \vec{n} are orthogonal while the highest permittivity, $\varepsilon_{r,\parallel}$, is observed when \vec{E}_{RF} and \vec{n} are parallel to each other. Bottom figure: Schematic illustration of the corresponding phase shift achieved by applying bias voltage leading to the change in permittivities. This figure illustrates that the achievable phase shift depends on the operating frequency f and temperature T .

Insertion loss: The interaction of the RF wave with the RIS circuit introduces a certain insertion loss, L_{ins} , which depends on the design as well as material properties such as dielectric losses, $\tan \delta$, and conductor losses. For the PhA implementation (see Section II-B), the phase-shifter length l_{PS} has a direct impact on the final insertion loss and maximum phase shift, see Fig. 3. In fact, increasing the phase-shifter length yields a higher maximum phase shift $\Delta\theta_{\max} \propto l_{\text{PS}}$ at the cost of a larger insertion loss $L_{\text{ins}} \propto l_{\text{PS}}$.

Clearing point temperature: Another physical property of LCs is the temperature at which an LC phase is converted to an isotropic liquid. This temperature is known as the clearing point, T_c , after which tunability is no longer possible, and hence constitutes the highest operation temperatures. From the material design perspective, the main targets of LC design is to achieve high phase-shift contrasts, $\Delta\varepsilon$, low dielectric losses, $\tan \delta$, high clearing point temperatures, T_c , and fast response times by reducing the rotational viscosity of the molecules, γ_{rot} . The values of these parameters for several commercially available LC mixtures are shown in Tab. I.

B. LC-based RIS implementation

Next, we first discuss the basic components that are required to realize an LC-RIS. Subsequently, we introduce two implementation approaches of LC-RISs, namely the RA and PhA methods, and discuss their advantages and limitations. Both implementations are potentially compatible with current LCD technology, which is a great advantage for the realization of cost-effective large RISs, see Fig. 3.

Basic components: The thin LC layer is usually placed between two layers of glass. The choice of glass over more

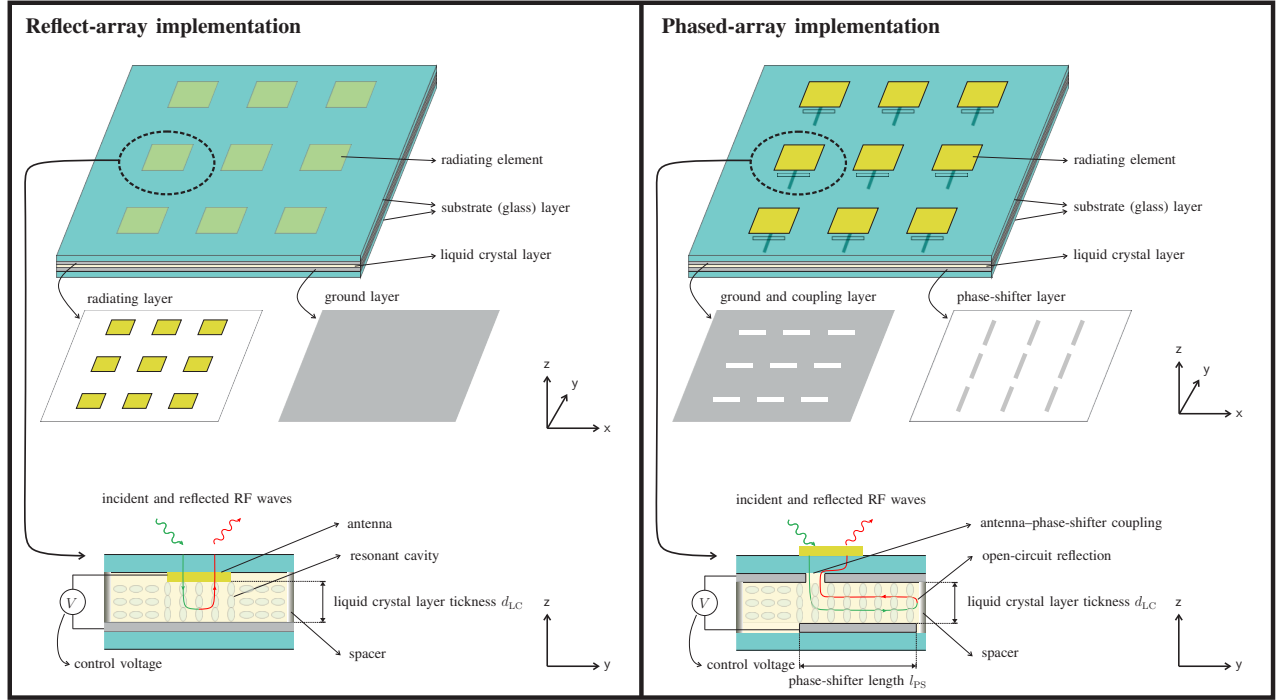


Fig. 3. Schematic illustration of reflect-array vs. phased-array LC-RISs. The top figures illustrate the implementation of LC-RISs in three dimensions whereas the bottom figures show a single unit cell from $y - z$ cross-section. The different layers, propagation path of the RF wave, and important design parameters such as phase-shifter length l_{PS} (influencing the maximum phase-shift and insertion loss) and LC-layer thickness d_{LC} (impacting the RIS response time) are schematically illustrated.

TABLE I
LCs FOR MM AND SUB-MM WAVE BANDS AND THEIR MATERIAL PROPERTIES. [10]

LC	$\epsilon_{r,\perp}$	$\tan \delta_{\perp}$	$\epsilon_{r,\parallel}$	$\tan \delta_{\parallel}$	$\Delta\epsilon$	$T_c (^{\circ}\text{C})$	K_{11} (pN)	γ_{rot} ($\text{Pa} \cdot \text{s}$)
K15 (5CB)	2.7	0.0273	3.1	0.0132	0.4	38.0	7.0	0.126
GT3-23001	2.41	0.0141	3.18	0.0037	0.77	173.5	24	0.727
GT5-28004	2.40	0.0043	3.32	0.0014	0.92	151.0	11.8	5.953
GT7-29001	2.46	0.0116	3.53	0.0064	1.07	124.0	14.5	0.307

common materials is due to the fact that a very thin LC layer with a well-defined thickness needs to be achieved over large panels, therefore a stiff, smooth solid substrate is needed. Due to its liquid state, solid spacers are needed to maintain the desired LC layer thickness. Moreover, the circuits of planar LC are commonly grown directly on glass substrates. Thereby, one or both sides of each glass are selectively metalized to pattern the desired circuitry, e.g., control lines and biasing electrodes. In particular, one of the glass substrates is often metalized to act as a ground layer for biasing all unit cells, whereas the other glass is selectively metalized for introducing phase-shifting control voltage of individual unit cells, see Fig. 3. To receive and re-radiate the phase-shifted signal, a radiating element is needed, usually a patch or a dipole antenna.

Reflect-array implementation: In this method, there is a common ground for all RIS elements and the LC layer is directly between the antenna (acting also as one of the biasing electrodes) and the ground, see Fig. 3. This structure forms a resonant cavity between the metal patch and the uniform ground plane. The advantage of this design is its simplicity since no patterning of the ground plane is necessary and

therefore only the layer with the patches must be etched. This avoids any alignment issues during assembly. However, the limitations of this method are: *i)* Due to the resonant effect, there is a limited bandwidth at which a nearly constant group delay and low amplitude variations can be achieved. *ii)* Thicker LC layers, d_{LC} , are needed to support wideband resonances with a low radiation quality factor to minimize the losses. This results in slow response times, $\tau_{\text{off}} \geq 10\text{s}$. *iii)* The LC biasing lines are comprised in the same layer of the patches and therefore need to be considered in its design. As a guiding value, such designs achieve impedance bandwidths² below 10% and insertion losses in the range 6 to 10 dB.

Phased-array implementation: In this method, one of the glass substrates is metalized such that each RIS element has a dedicated phase shifter (i.e., a biasing electrode). Moreover, the ground layer is patterned to couple the radiating elements to the phase-shifters, see Fig. 3. For the realization of the phase shifters, transmission line topologies compatible with LCD manufacturing are needed. One of these transmission

²The range of frequencies over which the antenna has an acceptable (-10 dB) impedance matching.

lines is the Inverted MicroStrip Line (IMSL) which is depicted in Fig. 3. The transmission line should be terminated with a reflective end. A suitable solution is the abrupt termination of the metal strip in an open end. Although such an open-end shows increased undesired radiation, this radiation is mainly proportional to the thickness of the LC layer, d_{LC} . Small $d_{LC} < 100 \mu\text{m}$ hence minimizes this effect. The advantages of the PhA method are: *i)* bandwidth is not limited by the phase shifter, and a thick glass in the radiating layer allows a wideband radiating element. A nearly constant group delay and low amplitude variations across the bandwidth can be achieved. *ii)* Thin LC layers, d_{LC} , are possible and lead to response times, $\tau_{\text{off}} < 100 \text{ ms}$. *iii)* The LC biasing lines are comprised in an additional layer. They do not disturb radiation, but additional processing steps are needed to metalize and pattern the additional layer. The insertion loss of the phase shifter for thin d_{LC} , specifically $4.6 \mu\text{m}$, is determined to be 4.5 dB for full 360° tunability at 28 GHz in [9]. The matched impedance bandwidth is expected to range around 15 %.

III. COMPARISON OF TECHNOLOGIES FOR BUILDING RISs

From a broad perspective, there are three main technologies for realizing a RIS, namely LC, SC, and MEMS. In this section, we provide an overview of each method and discuss the respective advantages and limitations.

A. LC-based RISs

The fundamentals of LC-RISs have been discussed in detail in the previous section, hence we elaborate on the advantages and limitations of this technology.

Advantages: One of the key merits of LC-RISs is *scalability at low-cost*. LC has been used for standard LCD fabrication processes for decades. Therefore, the production of large LC panels is technologically both very accessible and inexpensive. The cost of LC-RISs can be even less than LCD displays due to the lower number of *pixels*, the lack of backlight, as well as the larger tolerances compared to, for example, the strict color accuracy standards applied to displays. The other advantage of LC is its *low power consumption*. Due to its dielectric nature, LC experiences minimal current flow only to alter its state, specifically for rotating the LC molecules. Nonetheless, this power requirement is significantly lower compared to other technologies such as PIN diodes. The other important feature of LC is the *continuous tuning* capability, which is useful when sophisticated wavefront shaping (beyond a simple narrow reflection beam) is required, e.g., to reduce interference in multi-user systems.

Limitations: Despite major advances in LC microwave community, the response time of these devices are still higher than SC and MEMS (e.g., $> 10 \text{ ms}$ for PhA and $> 10 \text{ s}$ for RA). This implies that while the RISs are able to adapt to the user movement (e.g., on the order of seconds), they cannot adapt to fast fading. In addition, LC-RISs are suitable mainly for high frequencies $> 10 \text{ GHz}$ and cannot be adopted for sub-6 GHz communication systems featuring rich multi-path environments. Moreover, the phase-shifting behavior of LC-RISs is temperature-dependent, see Fig. 2, which necessitates

the adaption of reconfiguration strategy for the environments with significant temperature variations, see Section IV-C for possible solutions.

B. SC-based RIS

SCs are very common for PhA antennas. Similar designs have been leveraged in prototyping RISs. Under this category, there are two common approaches, namely PIN diodes and varactors.

A PIN diode is a low-capacitance device with high-frequency switching capabilities. By toggling between low and high-resistance states, the reflected wave's phase can be switched between two discrete states, typically 180° apart. Conceptually, RF-switches are similar to PIN diodes, as they are most commonly built as a packaged network of PINs. Varactors, on the other hand, have more significant capacitance variations and can be continuously tuned, but this higher capacitance also limits their maximum operation frequency.

Advantages: SCs are readily available at increasingly higher frequencies. Furthermore, SC-RISs offer low insertion loss, fast switching speeds below a μs , and compact size.

Limitations: The high power consumption (varactors, several PIN diodes) and pronounced temperature sensitivity are some of the technical disadvantages to be considered. However, the main factor is that the cost of building a SC-RIS rises quadratically with the surface area due to the increasing number of diodes required (one diode per bit and radiating element). Despite continuous advances in packaging, reliably and cost-effectively integrating thousands or even millions of discrete RF-components in large surfaces still poses a challenge. This remains an issue as long as the components cannot be selectively grown in the wafer, as is the case of the Thin-Film Transistors (TFTs) used for LC biasing, see biasing challenges in Section IV-E. The main limitation of using the diodes or transistors as the RF tuning element is that they need to operate at the RIS operating frequency, which poses an extremely high demand on the processing capabilities.

C. MEMS-based RIS

From a high-level perspective, MEMS phase shifters are structures whose electrically controlled micro-displacements result in phase shifts of the RF-fields propagating in the component. These solutions become relevant for high-frequency systems (mm-Wave and THz), where the wavelength is small and micro-displacements can lead to significant phase shifts. There are two different methods to use MEMS as RF-phase shifters: *i)* MEMS-actuated mirrors and MEMS switches. MEMSs-actuated mirrors that change their position in the direction normal to the surface of the antenna, varying the phase of the reflected wave; and *ii)* MEMS switches which are in principle tunable capacitors that rely on the controlled displacement of a conductive structure inside a transmission line, often referred to as a cantilever, with an applied voltage.

Advantages: MEMS-actuated mirrors have nearly negligible loss and are faster than LC, in the hundreds of μs range. MEMS switches share the advantage of faster tuning than LC.

TABLE II
COMPARISON OF TECHNOLOGIES USED FOR THE REALIZATION OF RIS.

	Varactor	PIN Diode	MEMS Switch	MEMS Mirror	LC
Tuning time	ns	ns	μ s	100s of μ s	> 10 ms
Tunability	continuous	discrete (1 bit/diode)	discrete	discrete	continuous
Power consumption	medium	medium	low	low	low
Scalability	low (cost per diode)	low (cost per diode)	medium (encapsulation)	medium (cost per area)	high
Frequency range	few GHz	mm-Wave	mm-Wave	THz	> 10 GHz
Cost	high	high	high	high	low
Example	[11]	[5]	[8], Ch. 4	[12]	[9], [13]

Limitations: For MEMS-actuated mirrors, the currently achievable maximum micro-displacement of e.g. 150 μ m limit the minimum frequency 1 THz when 360° phase shift is desired. Furthermore, their element dimension is currently larger than wavelength, thus the presence of grating lobes cannot be avoided. To overcome the instabilities of the displacements due to the involved non-linear forces, anchoring positions are usually used, which leads to discrete displacements in practical designs. Nevertheless, multiple-bit solutions exist such as [12] with 27 states (more than 4 bits). Finally, the fabrication and packaging is affected by the same cost limitation as SCs. Similar to actuated mirrors, the stability of MEMS switches limits the number of phase-shift states. In addition, the insertion loss of MEMS switches is in a similar range as LCs for the lower mm-Wave frequencies and increases with frequency.

A comparative summary of the advantages and limitations of the discussed RIS technologies are presented in Tab II.

IV. CHALLENGES AND FUTURE RESEARCH

In this section, we discuss some of the unique challenges of LC-based RISs from both system and hardware perspectives.

A. Applications with slow reconfiguration

One of the main limitations of LC-RISs is their slow response time. There are two key factors that impact the response time: the LC mixture and the LC layer thickness, i.e., $\tau_{\text{off}} \propto \gamma_{\text{rot}} d_{\text{LC}}^2$. The rotational viscosity of the LC, γ_{rot} , can be improved by using less viscous LC mixtures such as GT7 instead of GT5, but at the expense of increased dielectric losses. The LC thickness, d_{LC} , strongly depends on the adopted RIS implementation approach. In RAs, LC thickness is commonly on the order of 100 μ m leading to a response time on the order of tens of seconds. Due to the resonant structure in this approach, thinner layers would lead to a significant reduction in both the bandwidth, and an increase in the insertion loss. On the other hand, LC thickness in PhAs is thin as 4.6 μ m which yields a response time in the range of tens of milliseconds (e.g., 70 ms in [9]).

The above discussion suggests that RIS technology should be chosen based on the applications. For scenarios where the RIS configuration is static for an extended time period (e.g. for illumination of a blocked area), the LC-RISs with RA implementation are suitable due to relatively lower complexity and cost. For scenarios where continuous adaptation is needed (e.g., for illuminating mobile users/devices), then LC-RISs with PhA implementation may be a preferred choice. For

extremely fast reconfigurations (e.g., to track small-scale fading), other technologies such as SC-RISs are needed. Although for the latter case, the overhead of channel estimation and control signaling (rather than RIS response time) may be the bottleneck, in practice.

B. Undesired transient behaviour

Due to the slow response time, the reflection pattern of LC-RISs cannot be instantaneously reconfigured, which leads to potentially undesirable transient behavior. We show this transient behavior in Fig. 4 for the following case study. It is assumed that an incident wave is normally impinged on the RIS and then reflected first at $(\phi, \theta) = (-20, -30)$ and then at $(30, -20)$. For robustness and in order to reduce the reconfiguration overhead, wide beams of approximately 5 degrees are constructed using the quadratic phase shift design from [14]. Moreover, we show the Normalized RIS Cross-Section (NRCS) where the normalization is w.r.t. the maximum achievable gain by RIS (i.e., the peak of NRCS is 1 for specular reflection). The transition behavior is modeled by $\tau_{\text{off}} = 70$ ms and $\tau_{\text{on}} = 10$ ms (time where 90% of the phase-shift is achieved), which are taken from the PhA design in [9]. The RIS has a size of $50\lambda \times 50\lambda$, where λ is the wavelength.

Fig. 4 shows that the angular profile of NRCS (in dB) at time instances $t = 0, 10, 40, 70, 140$ ms. We can observe from this figure that the RIS reflects the wave in many directions within the transient duration, causing interference in unwanted directions. Therefore, an interesting direction for future research is to develop novel phase-shift configuration strategies that are aware of the RIS transient behavior. Example problems include the design of phase-shift schemes that minimize the time to reach the desired reflection pattern or keep the interference during the transient duration below a maximum level.

C. Temperature-adaptive RIS configuration

In an outdoor scenario, a RIS needs to withstand a large range of temperatures. For outdoor cellular systems, operation within -30°C to 50°C should be guaranteed. As is illustrated in Fig. 2, the phase-shift vs. control voltage curve of the LC-RIS is a function of temperature. This implies that a RIS phase-shift configuration that is designed for temperatures in summer may not be applicable in winter. Hence, there is a need to develop temperature-aware phase-shift strategies. This requires the RIS phase-shift behavior to be characterized offline

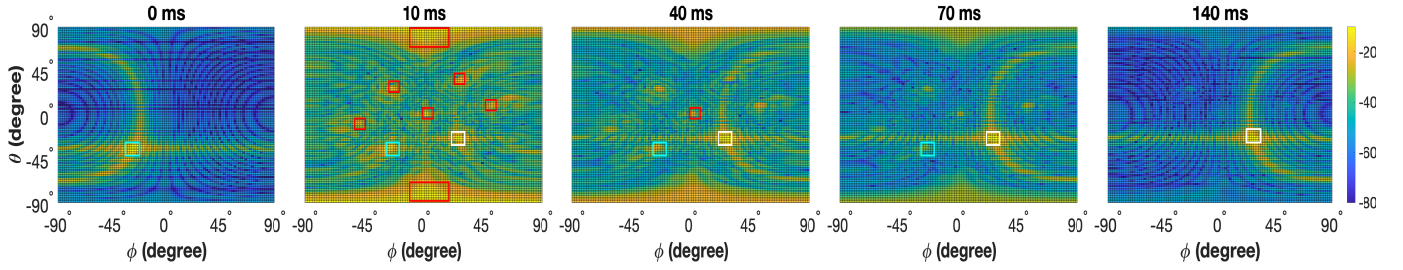


Fig. 4. NRCS (in dB) at several time instances when transitioning from desired reflection angles $(\phi, \theta) = (-20, -30)$ to $(30, -20)$. Cyan, white, and red rectangles are showing the current, desired, and interference directions, respectively. The RIS response time constants are for the PhA design in [9] and the phase-shifts are based on the quadratic phase-shift design in [14].

and the temperature to be estimated (e.g., by a thermometer deployed on the RIS) during online operation for adapting the phase-shift design policy. Depending on the estimation error and update frequency of temperature information, robust designs that are valid for a range of temperatures may be required.

D. LC-RIS Design Tradeoffs

In general, the maximum attainable phase-shift of LC decreases with increasing temperature or decreasing frequency (see Fig. 2) [15]. Therefore, to guarantee the full 360-degree phase shift tuneability, one should design the RIS unit cells for the maximum temperature and minimum operating frequency. This can be achieved in the PhA implementation by choosing a sufficiently large phase-shifter length l_{PS} (within the feasible range given the implementation constraints), since the maximum phase-shift scales with l_{PS} . However, as discussed in Section II-A, the insertion loss also scales with l_{PS} . Therefore, investigating the tradeoff among the maximum achievable phase shift, the resulting insertion loss, and the achievable performance (across the operating temperature and frequency) constitutes an interesting direction for future research. To the authors' knowledge, this effect is not being considered and reported in current LC-RIS designs.

E. Biasing

For the realization of large RISs, the use of glass as a substrate is of great advantage due to the compatibility with current LCD technology. As in commercial LCD displays, using TFTs at each RIS element to address them with $N + M$ (number of rows + columns) connecting lines instead of $N \times M$ (one line per element) is a meaningful approach to the challenge of biasing thousands or even millions of elements. The additional challenge compared to common LCDs is the higher capacitance of mm-Wave circuits due to their larger size, requiring larger TFTs. However, constraints might arise to minimize the effect of the bias lines in the RIS operation. This poses an additional challenge in the design of element-wise tunable RISs using the RA method, since the bias lines will affect the performance of the radiating elements. This is commonly solved by biasing lines perpendicular to the electric-field polarization which is only possible for single, linearly polarized operation. Dual polarization designs require

alternative solutions that account for the effect of the biasing lines when designing the radiating elements. In the PhA method, this is not an issue due to the separation of the phase shifters and the radiating elements in different layers.

F. Bandwidth

RISs can be designed to support a single service provider (i.e., limited part of the band); an entire frequency band (e.g., 5G 26.5 GHz to 29.5 GHz band), or even several bands, for example, the 28 GHz and 60 GHz. For high bandwidth systems, operating in a single band, the PhA implementation is more suitable compared to the RA. However, RA implementation is more suitable for multi-band operations due to the simplicity of their design. However, this comes at the cost of higher response time. Moreover, the phase-shift vs. voltage control curve of LC-RISs (see Fig. 2) changes across different frequencies within the band. Therefore, wideband phase-shift designs that exploit the frequency-dependent characteristics of the LC-RISs have to be developed.

V. CONCLUSION

This paper presented LC as an enabler technology for building extremely large RISs with continuous tuning capability, low power consumption, frequency scalability, and cost-efficient fabrication. However, these advantages come with the limitations such as slow response time and temperature dependencies. The basic physical principles of LC theory were reviewed and two important implementations of LC-RISs were introduced. Finally, LC-RISs were compared against competing technologies SC- and MEMS-RISs and several important open research problems on LC-RISs were presented.

REFERENCES

- [1] M. Di Renzo, A. Zappone, M. Debbah, M.-S. Alouini, C. Yuen, J. De Rosny, and S. Tretyakov, "Smart radio environments empowered by reconfigurable intelligent surfaces: How it works, state of research, and the road ahead," *IEEE J. Sel. Area Commun.*, vol. 38, no. 11, pp. 2450–2525, 2020.
- [2] X. Yu, V. Jamali, D. Xu, D. W. K. Ng, and R. Schober, "Smart and reconfigurable wireless communications: From IRS modeling to algorithm design," *IEEE Wireless Commun. Mag.*, vol. 28, no. 6, pp. 118–125, 2021.
- [3] J. u. R. Kazim, T. J. Cui, A. Zoha, L. Li, S. A. Shah, A. Alomainy, M. A. Imran, Q. H. Abbasi *et al.*, "Wireless on walls: Revolutionizing the future of health care," *IEEE Antennas and Propagation Mag.*, vol. 63, no. 6, pp. 87–93, 2020.

- [4] D. Berry, R. Malech, and W. Kennedy, "The reflectarray antenna," *IEEE Transactions on Antennas and Propagation*, vol. 11, no. 6, pp. 645–651, 1963.
- [5] W. Tang, M. Z. Chen, X. Chen, J. Y. Dai, Y. Han, M. Di Renzo, Y. Zeng, S. Jin, Q. Cheng, and T. J. Cui, "Wireless communications with reconfigurable intelligent surface: Path loss modeling and experimental measurement," *IEEE Trans. Wireless Commun.*, vol. 20, no. 1, pp. 421–439, 2020.
- [6] I. Alamzadeh, G. C. Alexandropoulos, N. Shlezinger, and M. F. Imani, "A reconfigurable intelligent surface with integrated sensing capability," *Scientific Reports*, vol. 11, no. 1, p. 20737, 2021.
- [7] M. Rossanese, P. Mursia, A. Garcia-Saavedra, V. Sciancalepore, A. Asadi, and X. Costa-Perez, "Designing, building, and characterizing RF switch-based reconfigurable intelligent surfaces," *arXiv preprint arXiv:2207.07121*, 2022.
- [8] P. Ferrari, R. Jakoby, O. H. Karabey, H. Maune, and G. Rehder, *Reconfigurable Circuits and Technologies for Smart Millimeter-wave Systems*. Cambridge University Press, 2022.
- [9] R. Neuder, D. Wang, R. Jakoby, and A. Jiménez-Sáez, "Compact liquid crystal-based defective ground structure phase shifter for reconfigurable intelligent surfaces," in *European Conf. Antennas and Propagation (EuCAP)*, 2023.
- [10] R. Jakoby, A. Gaebler, and C. Weickmann, "Microwave liquid crystal enabling technology for electronically steerable antennas in satcom and 5g millimeter-wave systems," *Crystals*, vol. 10, no. 6, p. 514, 2020.
- [11] Y. Tawk, J. Costantine, and C. Christodoulou, "A varactor-based reconfigurable filtenna," *IEEE Antennas and Wireless Propagation Lett.*, vol. 11, pp. 716–719, 2012.
- [12] L. Schmitt, P. Schmitt, and M. Hoffmann, "3-bit digital-to-analog converter with mechanical amplifier for binary encoded large displacements," in *Actuators*, vol. 10, no. 8, 2021, p. 182.
- [13] O. H. Karabey, A. Gaebler, S. Strunck, and R. Jakoby, "A 2-D electronically steered phased-array antenna with 2×2 elements in LC display technology," *IEEE Trans. Microwave Theory and Techniques*, vol. 60, no. 5, pp. 1297–1306, 2012.
- [14] V. Jamali, M. Najafi, R. Schober, and H. V. Poor, "Power efficiency, overhead, and complexity tradeoff of IRS codebook design—Quadratic phase-shift profile," *IEEE Commun. Lett.*, vol. 25, no. 6, pp. 2048–2052, 2021.
- [15] H. Tesmer, R. Razzouk, E. Polat, D. Wang, R. Jakoby, and H. Maune, "Temperature characterization of liquid crystal dielectric image line phase shifter for millimeter-wave applications," *Crystals*, vol. 11, no. 1, p. 63, 2021.

VI. ACKNOWLEDGEMENTS

This research was partly funded by the Deutsche Forschungsgemeinschaft (DFG, German Research Foundation) – Project-ID 287022738 – TRR 196 MARIE within project C09, by the mm-Cell project and the Collaborative Research Center 1053 MAKI, and by the LOEWE initiative (Hesse, Germany) within the emergenCITY center.

BIOGRAPHY

Alejandro Jiménez-Sáez is a Research Group Leader at the Institute of Microwave Engineering and Photonics (IMP) at the Technical University of Darmstadt (TUDa), Darmstadt, Germany. His research interests include RF components based on artificial and functional materials.

Arash Asadi (Senior Member, IEEE) is a Research Group Leader at TUDa, where he leads the Wireless Communication and Sensing Lab (WISE). His research interests include wireless communication and sensing and its application in beyond-5G/6G networks.

Robin Neuder is a Ph.D. student at IMP, TUDa, Darmstadt, Germany.

Mohamadreza Delbari is a Ph.D. student at the Resilient Communication Systems (RCS) Lab at TUDa, Darmstadt, Germany.

Vahid Jamali is an Assistant Professor leading the RCS Lab at TUDa, Darmstadt, Germany. His research interests include wireless and molecular communications.